Reprinted from INVESTIGATIVE RADIOLOGY, Vol. 3, No. 4, July-August, 1968
 Printed in U. S. A.

Intracranial Anatomy Visualized in Vivo by Ultrasound

WILLIAM J. FRY

Ultrasonic visualization in vivo of anatomic features of the ventricles, cisterns, sulci and major blood vessels of the brain and the internal surface configuration of the cranial vault of the rhesus monkey, using recently developed instrumentation incorporating omnidirectional scanning, relief presentation and computer control of transducer positioning, data handling and display parameters, is illustrated. Results are presented in cross-sectional views of the tissue. In this study the acoustic energy had access to intracranial structures via an opening in the skull, but traversed the intact scalp, thus achieving separation of the problems associated with the traversal of bone from those concerned with identification of interfaces detectable by examining pulses alone. A resolution capability of 1 mm and an accuracy of localization of ±0.5 mm are achieved. All definitive echoes in the echograms are identified, and quantitative comparison of the anatomic information obtained with brain atlases is presented. The analytic determination of length scaling factors and relative angular orientation values for the subject's ultrasonically–viewed tissue cross sections and those of an atlas are also illustrated.

THE PURPOSE OF THIS PAPER IS TO DEMONstrate what can be achieved with ultrasonic visualization of intracranial structures using modern sophisticated methods of scanning, echo data composition and echogram presentation.[3] The results were obtained without transmission via the skull through the intact scalp. Therefore, the results of this study suggest the limit of what might be approached in trans-skull operation, and also provide an appropriate basis for the interpretation of echogram information obtained with the skull intact. This latter aspect is important since, at the present stage of development of ultrasonic visualization methods for viewing intracranial anatomy, it is difficult to identify the structures from which many observed echoes arise. For example, investigators have reported definitive echoes from ventricular boundaries, bone surfaces and gray–white matter interfaces, but the fractions of incident acoustic energy that can be received from these various borders are not of the same order of magnitude; thus, identifiable echoes cannot be elicited with equal facility from all of them. The relative degrees of difficulty are apparent from the results reported here.

A number of investigators feel that the development of ultrasonic instrumentation to provide cross-sectional "pictures" of the anatomy of the intracranial contents is complicated considerably by the presence of the skull. This concern is evidenced in the number of different types of equipment devised for compound scanning and presentation that provide useful information via the intact skull.[4] Of course, if ultrasonic visualization is to be valuable for routine examination of the human brain, the skull must remain intact. It is equally important that methods for the examination of intracranial structures not be restricted to detection and localization of only a small fraction of the surface area of the ventricular and cisternal systems and the bony interfaces.

From the Interscience Research Institute, Champaign, Ill.

Supported by PHS grant CA 07043 from the National Cancer Institute and research grant 407-1 from the National Multiple Sclerosis Society.

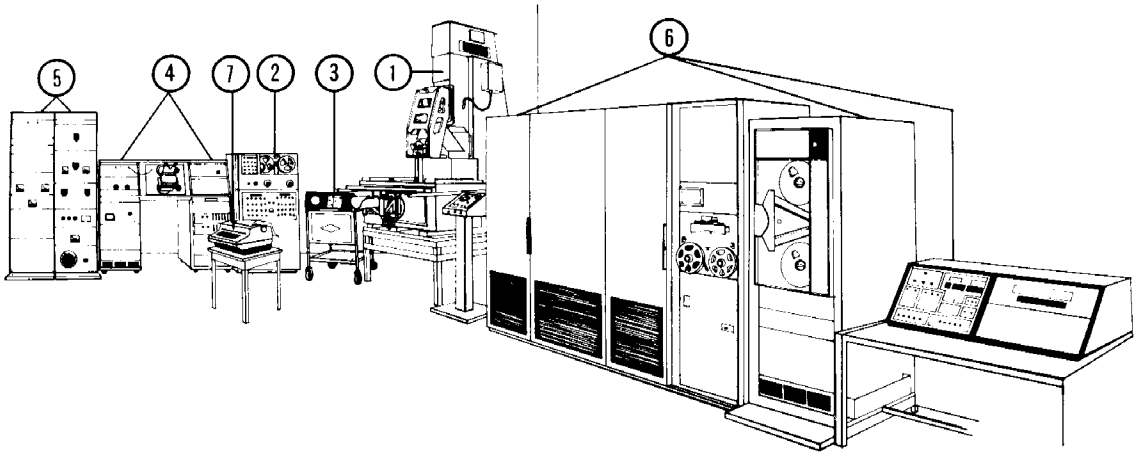

FIG. 1. *Major components of ultrasonic visualization facility.* (1) Apparatus for positioning and moving acoustic scanning assemblies and sound tank—positioning unit is a modified Turret Drill—Cintimatic model DE; (2) Electronic control unit for positioning machine—Cincinnati Acramatic 330; (3) Reflectoscope—Sperry model UM721—used during various acoustic alignment procedures as well as *on line* as part of the video channel for the system; (4) Console housing: visual display instrumentation, digital timers, digital to analogue converter units, and power supplies; (5) Electronic driver for ultrasonic transducers; (6) Digital computer—Raytheon 520—used on-line to control scanning motions and position, amplifier gains, echo signal processing, video display, and time sequences; (7) Typewriter for data input (Fortran language) and printout from the computer.

Normal intracranial anatomy that might be visualized by ultrasonic methods includes boundaries of the ventricles and other cisterns, configurations of the sulci, shapes of surfaces abutting or juxtaposed to the bones of the skull, major blood vessels and gray–white matter boundaries. Abnormal structures that might be seen include cysts, regions of extravasated blood, surface detail and internal features of tumors and aneurysms. A useful approach to the acoustic detection and localization of these structures would be to determine the possibility of identifying them without the complication of trans-skull operation. The difficulties posed by skull transmission lie in a different category than those associated with the detection, composition, and interpretation of echo information in general. To some extent other investigators have recognized that it is fruitful to separate these two aspects of the development of ultrasonic diagnostic methods for the examination of the intracranial contents.[5, 7]

Although problems of trans-skull operation are not considered here, it is worthwhile to mention the difficulties that impose limitations on echo information obtainable by approaches that necessarily have been employed first. The difficulties arise because of the magnitudes of the acoustic absorption coefficient and speed of sound in the skull. The sound velocity, higher than that in soft tissue, and the nonuniformity of the skull cause gross displacements in orientation by refraction of ingoing pulses and outgoing echoes. For some angles of incidence of the examining pulses the acoustic energy is totally internally reflected. In addition, ghost echoes may appear as the result of multiple internal reflections in the bone. The high absorption in the skull implies that the ratio of the amplitudes of the examining pulses to returning echoes is much larger than when soft tissue is examined without the interference of bone. Consequently, acoustic coupling to the subject and the maintenance of a safe dosage factor are more difficult.

Methods

Our results were obtained from an in vivo study on the rhesus monkey—*Macaca mulatta*—employing an instrumentation facility described in a paper now in press.[3] The information is displayed in two-dimensional echograms, employing a *relief* presentation which provides unique advantages

over *flat* displays. Echograms of single tissue cross-sections obtained by omnidirectional compound scanning, implemented by an on-line digital computer, are combined in composite pictures of echoes received from interfaces over a wide range of angular orientations with respect to the plane of section.

Pertinent characteristics of the instrumentation and methodology for the examination of intracranial anatomy by pulsed ultrasound have been described.[3] Fig. 1 shows the overall facility. Seen in the figure are:

1. A large positioning machine for moving the transducer array in the sound tank—the head fixation apparatus is coupled rigidly to this tank;
2. A unit for automatic control of the positioning machine;
3. An A-scope monitor unit;
4. Display equipment with synchronization and control circuitry and amplifiers for handling returning echo information—the viewing screen can be photographed for permanent records and data processing;
5. Electronic drivers that provide high power excitation for the transducers;
6. A digital computer with its control console;
7. A typewriter input for communication with the computer—the typewriter is placed at the display console so that a single operator can control the entire facility.

Integral parts of the system not shown include a still, a tank, associated pumps and a heat exchanger for producing, storing and transferring the degassed coupling medium to the sound tank, and hydraulic pumping units for moving the positioning unit. These facilities are in a separate room.

All the animals in our series underwent craniectomy to provide a bone-free window which places the dorsal and lateral aspects of the brain adjacent to overlying muscle and scalp. This procedure is performed so that the animal has recovered completely and the scalp is healed before ultrasonic examination is scheduled. The opening permits examination of intracranial anatomy over a wide range of relative angular orientations of the beam axis and the axes of the head.

The experimental animal is anesthetized before acoustic examination. Its head is shaved and placed in the supporting structure, which is rigidly coupled to the sound tank. This is a Clarke's support[2] which is modified for rotation (30° range) of the animal's head about the axis through the ear bars (Fig. 2). This rotational degree of freedom provides an angular motion necessary for omnidirectional scanning. The animal's head is

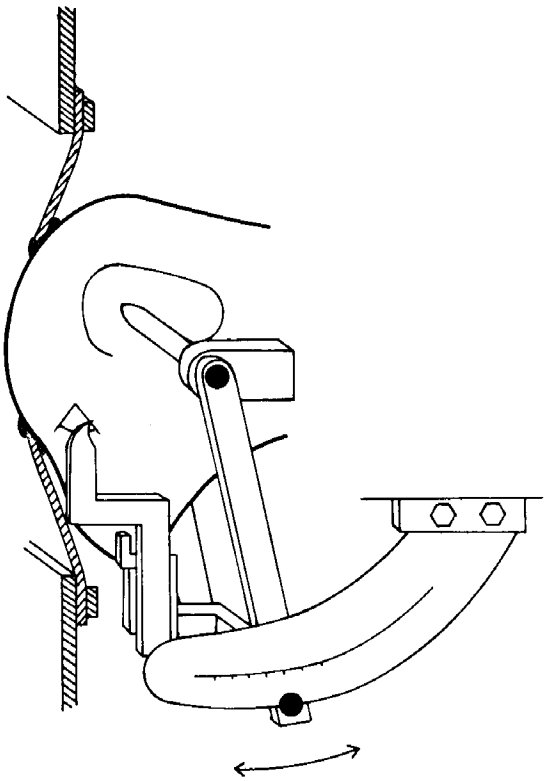

FIG. 2. Configuration of head-supporting structure and coupling of scalp to sound tank.

placed against the flexible diaphragm; a caulking compound at the rim of the opening makes a watertight seal with the scalp. The head support is used as the reference coordinate system when ultrasonic echograms of brain cross-sections are compared with atlas sections.[1, 6]

For flexibility, we employ a large sound tank containing the degassed liquid, which transmits acoustic energy from the transducer assembly to the subject. In the configuration illustrated in Fig. 3, a lucite window supports the coupling diaphragm. The oval opening in the diaphragm conforms approximately to the shape of the top of the animal's head. No appreciable leaking occurs over many hours with a water pressure head of 15 cm when the sealant is used and the animal's head is simply pushed into the diaphragm. Coupling and decoupling of the subject require only a few minutes.

The shape of the transducer assembly is indicated in Fig. 3. Separate piezoelectric elements produce and receive the pulsed acoustic radiation, characteristics of which have been described.[3] Outgoing pulses are produced by a transducer unit (2.5 cm diameter) at the forward end of the

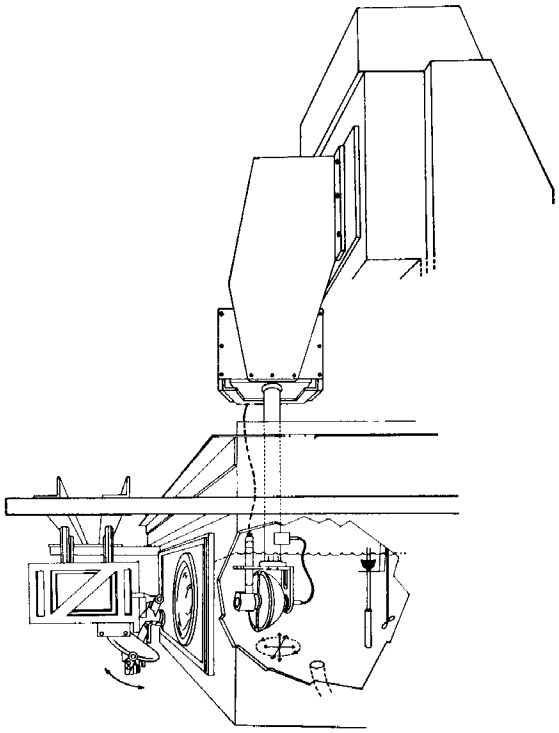

FIG. 3. Arrangement of head fixation apparatus, sound tank, transmitting liquid, transducer assembly, and column of positioning machine.

assembly, while the returning radiation is collected by a reflector (14.0 cm diameter) which brings the energy via a second reflector, to focus on a small (3 mm diameter) unit placed at the rear of the assembly. Range resolution is controlled by the acoustic pulse length and receiver amplifier properties. The beam pattern characteristics of the reflector assembly and the same amplifier determine azimuthal resolution. Range and azimuthal resolutions of 1.0 mm each are achieved readily in the focal region of the transducer assembly, as is apparent from the echograms. A coaxial line—indicated in the forward part of the transducer assembly—supplies electric excitation for the transmitting unit. Returning electric signals from the receiving unit are transmitted to an adjacent preamplifier via a short coaxial lead which enters the transducer assembly at the rear. The sound tank contains temperature-sensing and heating elements and a stirring unit to prevent temperature gradients of more than 1 C°. Pumps circulate the degassed liquid through a heat exchanger on its way to the tank.

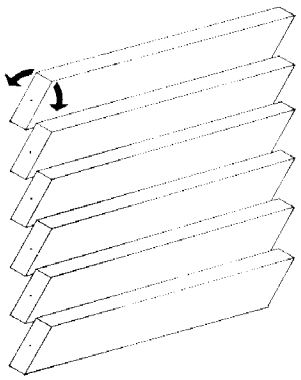

FIG. 4. Group of tissue *slats* corresponding to a single planar cross-section through the tissue under examination, from which echoes are received when the examining beam axis is not within the plane of section.

Scanning in sections of the intracranium is made possible by the motions provided on the positioning system, as indicated in Fig. 3. The three rectilinear directions of movement and single rotary motion of the transducer assembly are indicated by the diagram at the base of the transducer assembly. The range of movement provided by the positioning system places the head of the subject in any desired position. The examining beam axis can be rotated in the plane of sector-scanning 20° from the mid-position, that is, the total range of rotation during automatic scanning is 40°. In addition, the mid-position of the beam axis can be tilted 45° from its projection in the midsagittal plane.

Omnidirectional compound scanning is not achieved by taking a number of sets of planar sections making different angles with axes fixed with respect to the head. First, a series of planar pictures is taken throughout the brain, or that fraction of it to be examined, for a single angular setting of the head-holder fixture. Then planar echograms of the same tissue sections are constructed with the head support in other angular positions. Construction of such echograms is accomplished by program control, adjusting with the computer the positions of the transducer assembly and the gating circuits of the presentation system, so that echoes from essentially only the tissue cross-sections first examined are displayed, that is, for one angle setting the echoes seen in a single echogram are from a set of tissue *slats* (Fig. 4). Usual compound scanning methods detect only echoes indicated in the first series of pictures, that is, those with the examining beam axis in the plane of section. The range intervals recorded on the echograms, as indicated by the width of the slats in Fig. 4, was adjustable, for the work reported here,* from 7 mm to the entire width of the picture—50 mm. To achieve maximum resolution in examining each slat, the center of the focus of the transducer assembly is placed at the approximate center of the width of the slat.

The on-line computer can control the gain of the receiver amplifier so that it is optimal for the

* This range is now adjustable to one mm.

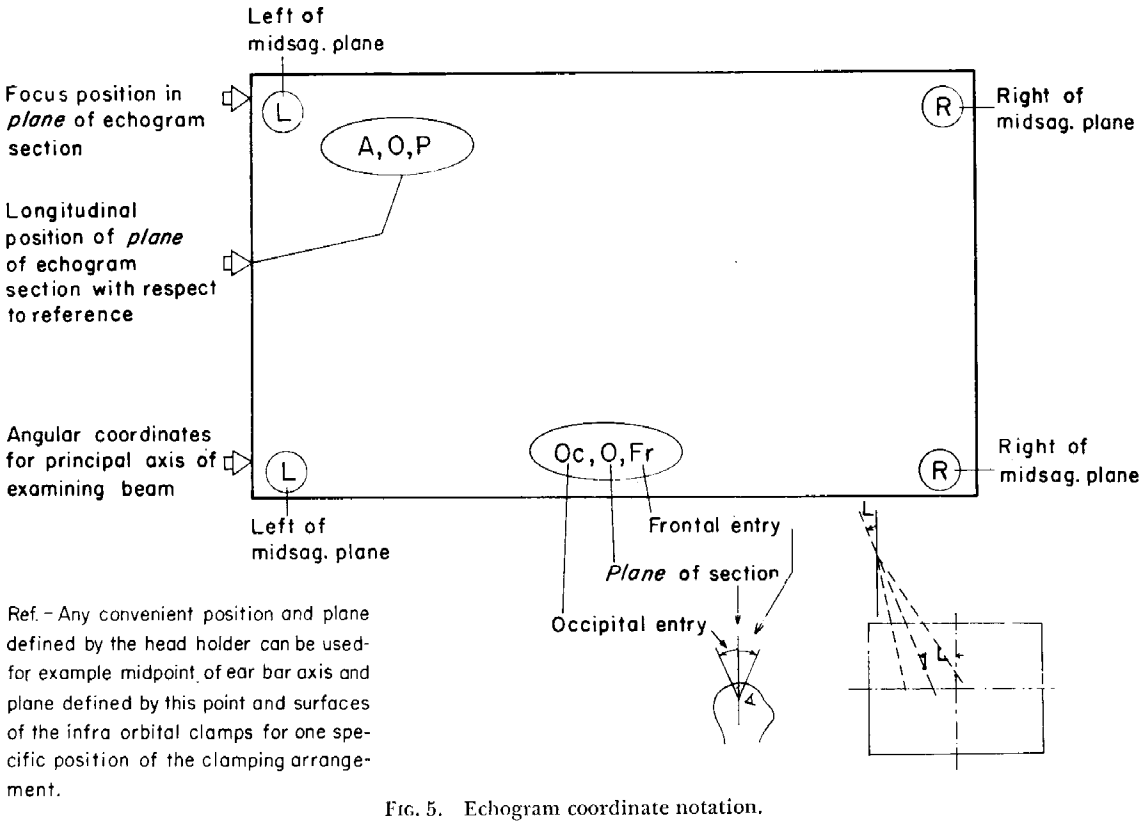

FIG. 5. Echogram coordinate notation.

range interval on the echogram.† This is a major step toward achieving high resolution combined with wide dynamic range over the entire echogram since the amplifier gain can be set to display only those echoes received within a certain range interval, that is, for a specific range of depths in the tissue. Of course, the time-variable gain requirements imposed on the receiver amplifier in the usual visualization system are eliminated—that is, absorption loss and beam spreading are offset by program control, with the resolution advantages of a linear amplifier.

The echograms are photographed on a scale of one to one, that is, anatomic spacing intervals are maintained on the echograms. This makes it convenient to compare measurements made on the echograms with coordinate differences obtained from brain atlases, stained tissue sections, and skulls.

Echogram Terminology

It is essential in labeling echograms to indicate the plane of tissue section and the rectilinear and angular coordinate values employed to place the focus of the examining beam and its principal axis in the plane of section during sector scanning. Although individual echograms can be constructed in which compound scanning is employed directly, that is, sector scanning combined with a rectilinear or other movement of the transducer system, it has been appropriate in these studies to make photographic records of the echo information obtained for each sector scan. Fig. 5 summarizes the notation; the symbols are shown in the positions occupied on the echograms.

The position of the tissue cross-section corresponding to the echogram along the anteroposterior axis of the head, at the level of the horizontal reference plane, is designated in the upper left hand corner of the echogram; A indicates positions anterior to the ear bar axis, and P indicates posterior positions. An angular coordinate value in degrees indicates the orientation of the principal axis of the beam with respect to its projection in the plane of the echogram. It appears in the center of the lower row of symbols with the diagram below it serving to define the symbols. (Zero indicates that the axis lies in the *plane* of the echogram and Oc and Fr designate, respectively,

† Program control of the gain within each range interval is now being incorporated.

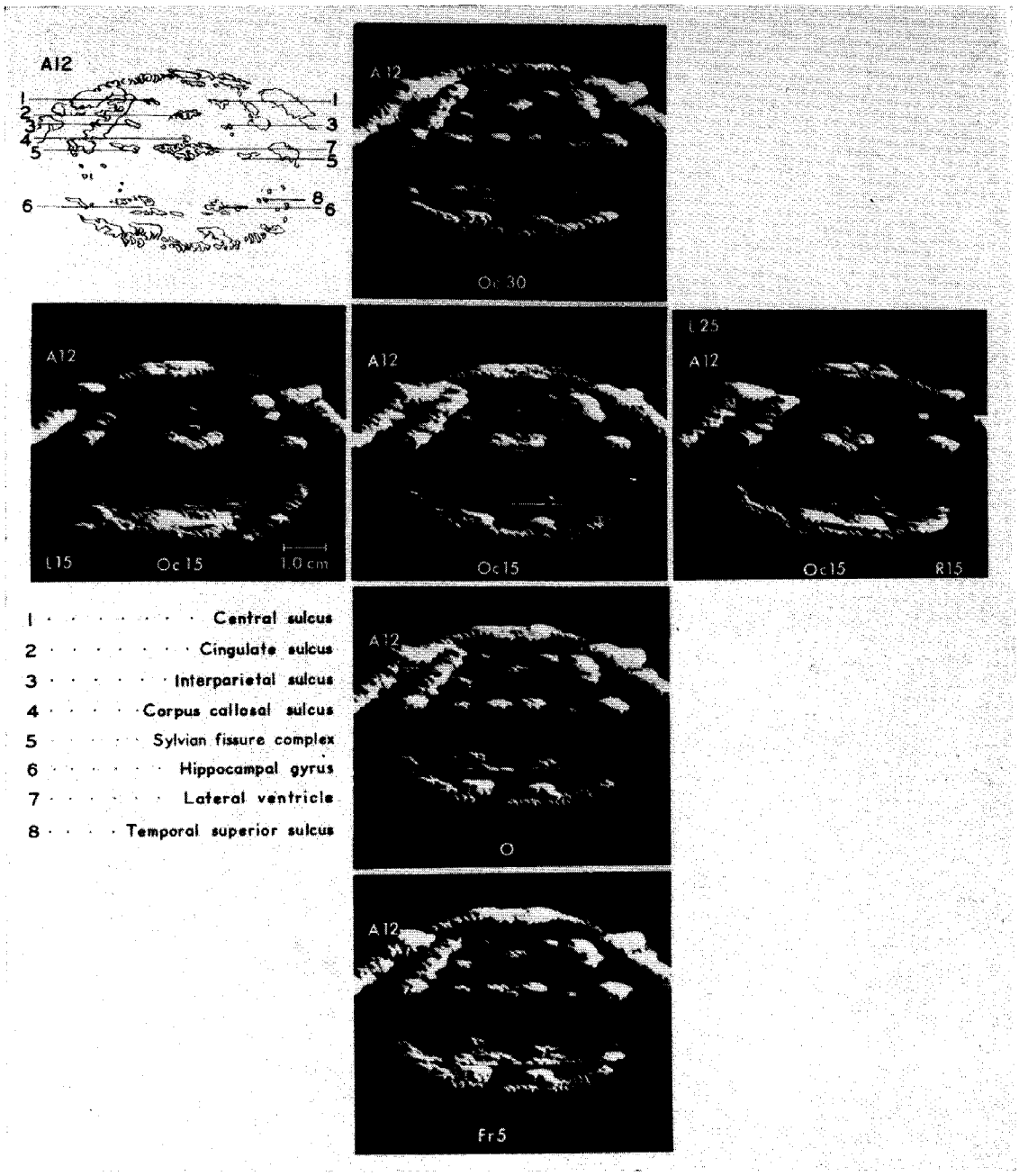

FIG. 6. Composite echogram (upper left) constructed manually from information from the six accompanying echogram photographs. Vertical column of echograms obtained for different positions of rotation of the animal's head about the ear bar axis. Horizontal row of echograms is for different orientations of the examining beam axis with respect to the midsagittal plane, (axis remains in the same transverse plane). Chart identifies anatomic features manifested in the composite echogram.

occipital and frontal entry of the examining beam axis with respect to the plane of the tissue section.) The other symbols on the bottom of the echogram designate the angular orientation of the principal axis of the examining beam with respect to the midsagittal plane; deviation to the left by L (illustrated by the diagram in the lower right hand corner of the figure) and to the right by R. The symbols at the top of the echogram indicate the rectilinear coordinate position of the center of the focal region of the transducer assembly in the plane of the echogram; displacements in millimeters to the right or left of the midsagittal position are indicated by R and L, respectively.

Five coordinate values must be designated for each band of information on the echogram.‡ The dorsoventral position of the focus is not listed on the echogram—five to seven values, i.e., one for each band, were employed for the pictures illustrated in this paper.

Echogram Composition

Although echograms incorporating all information obtained from omnidirectional scanning of a specific tissue cross-section can be constructed automatically and recorded directly on film, it has been fruitful to record a series of individual echograms for each pair of values of the angular coordinates of the beam axis and for each lateral coordinate position of the transducer assembly. The advantage of this is that various criteria for combining echo information can be tested, and the results serve as a basis for later automatic programming. The magnitude and importance of registration differences are apparent immediately. These differences show the extent of corrections in the instrumentation necessitated by relative displacements caused by refraction and transit-time differences, before automatic composition is possible.

An example of the manual method of composition is illustrated in Fig. 6. It was constructed by transferring data from individual echograms successively, onto a plastic overlay. To implement this method a transparent plastic sheet is placed over one of the echograms and a drawing transfer of the echographic information is made to this sheet. Then the overlay can be superimposed over a second echogram and registration accomplished for elements of the picture and diagram by the common structures which they both display. Then transfer of the non-common echo information to the overlay is made. Registration for a second element of area is accomplished, and the process repeated until all pertinent information has been transferred. By repeating this process with the other echograms, it is possible to collect all significant echo information from the entire series.

The composition process is accomplished without reference to an atlas of brain cross-sections. Identification of specific echoes with anatomic features is apparent immediately for much of the pattern information following examination of a series of the pictures. A principal advantage of an atlas is that it provides an annotated reference before an examiner has accumulated experience in the interpretation of echograms, in particular the pattern information of the sulci in cross-section. An atlas is also useful in quantitative stereotaxic work on the brain.

It is understood that in labeling features on the composite, the tip of the line in each case refers to the group of echoes in its immediate neighborhood and not, in general, to a single one. Most interfaces are not represented as a connected series of echoes because of the relative orientation of its incremental elements of area and the examining beam axis.

That the composite more completely represents the anatomic features within the section of the brain under examination than any of the individual echograms is apparent.

Although time-consuming, the manual method could be used to produce echograms that contain all echo information obtainable for a series of closely-spaced positions throughout an entire brain. The manual method is particularly useful for demonstrating the methodology, and for acquiring knowledge to formulate program criteria and instrumentation specifications for the automatic composition of echo data. Subjects are examined by obtaining for each, first a series of closely-spaced echograms, each corresponding to a single sector scan, followed by detailed studies of a few specific sections using the more comprehensive scanning methods.

Results and Discussion

Echograms of transverse cross-sections exhibit intracranial anatomic information obtainable by using the visualization facility developed by the author and collaborators. A series of echograms obtained by simple sector-scanning—principal axis of the beam in the plane of section—is taken at intervals of 1.0 mm throughout most of the anteroposterior extent of the rhesus brain. Other series of echograms illustrate results for single cross-sections examined for various orientations of the principal axis of the examining beam, within the plane of section and with respect

‡ Each band corresponds to a slat of tissue as illustrated in Fig. 4.

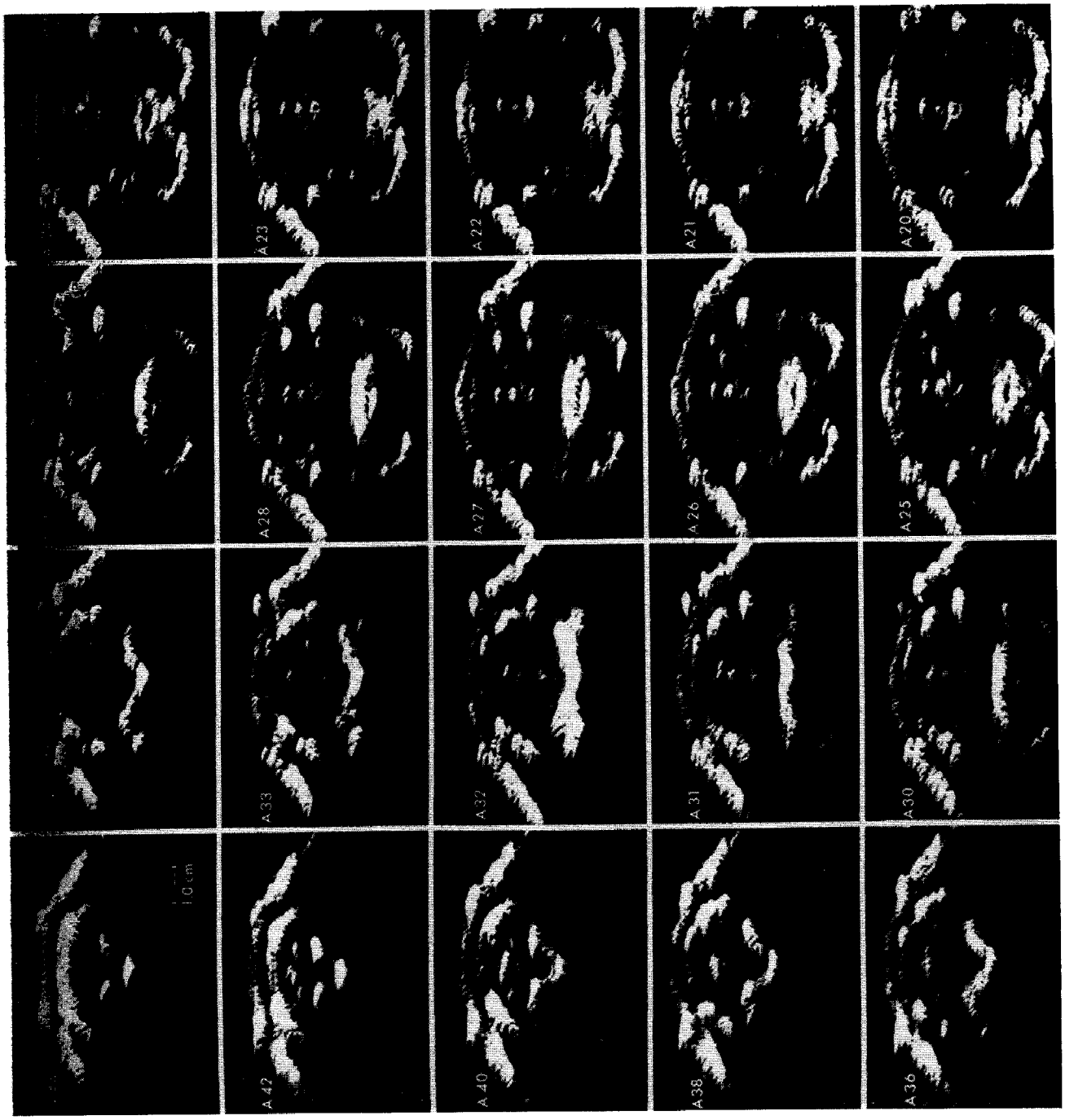
A23
A22
A21
A20
A28
A27
A26
A25
A33
A32
A31
A30
1.0 cm
A42
A40
A38
A36

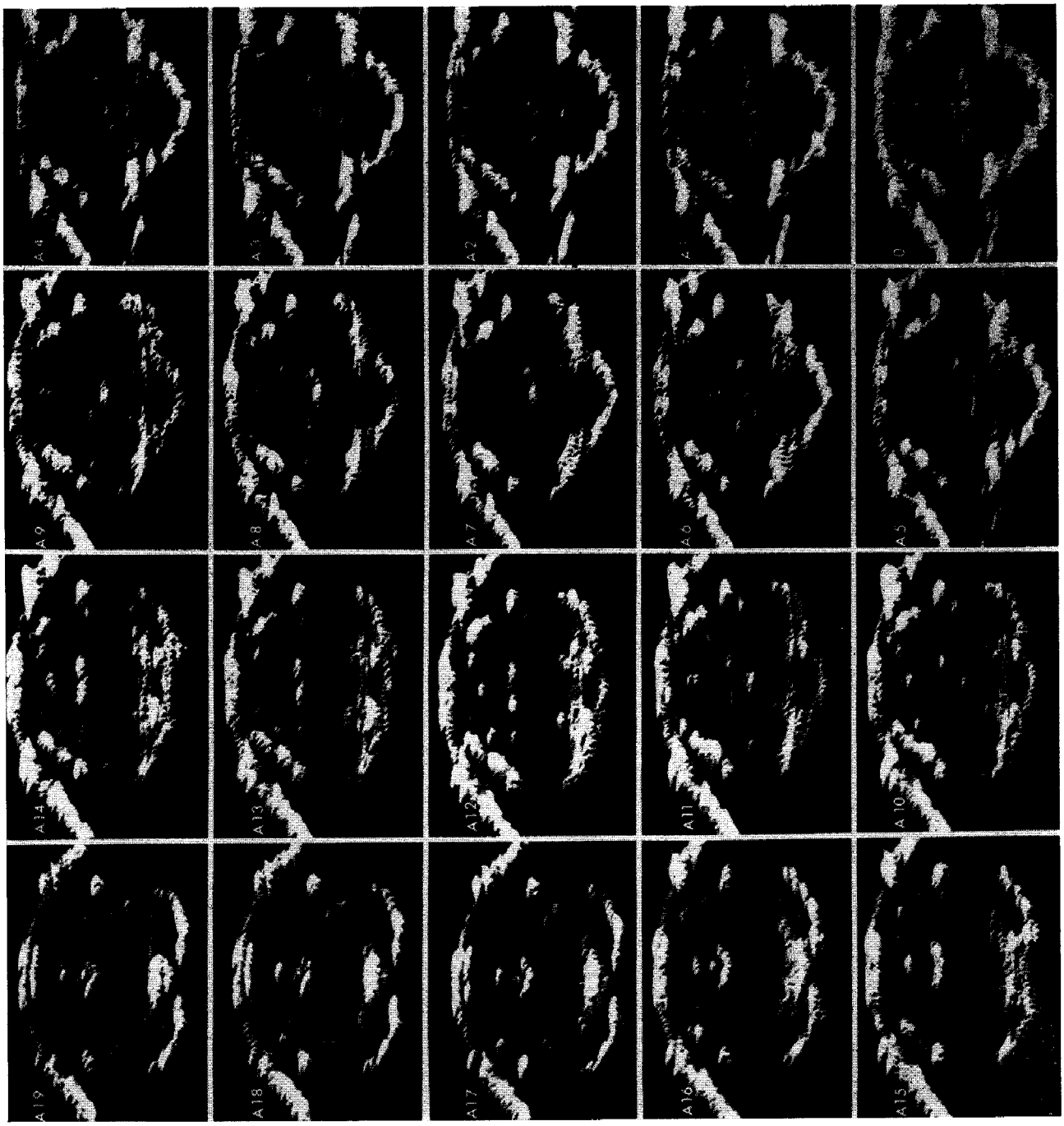

(See page 252 for legend)

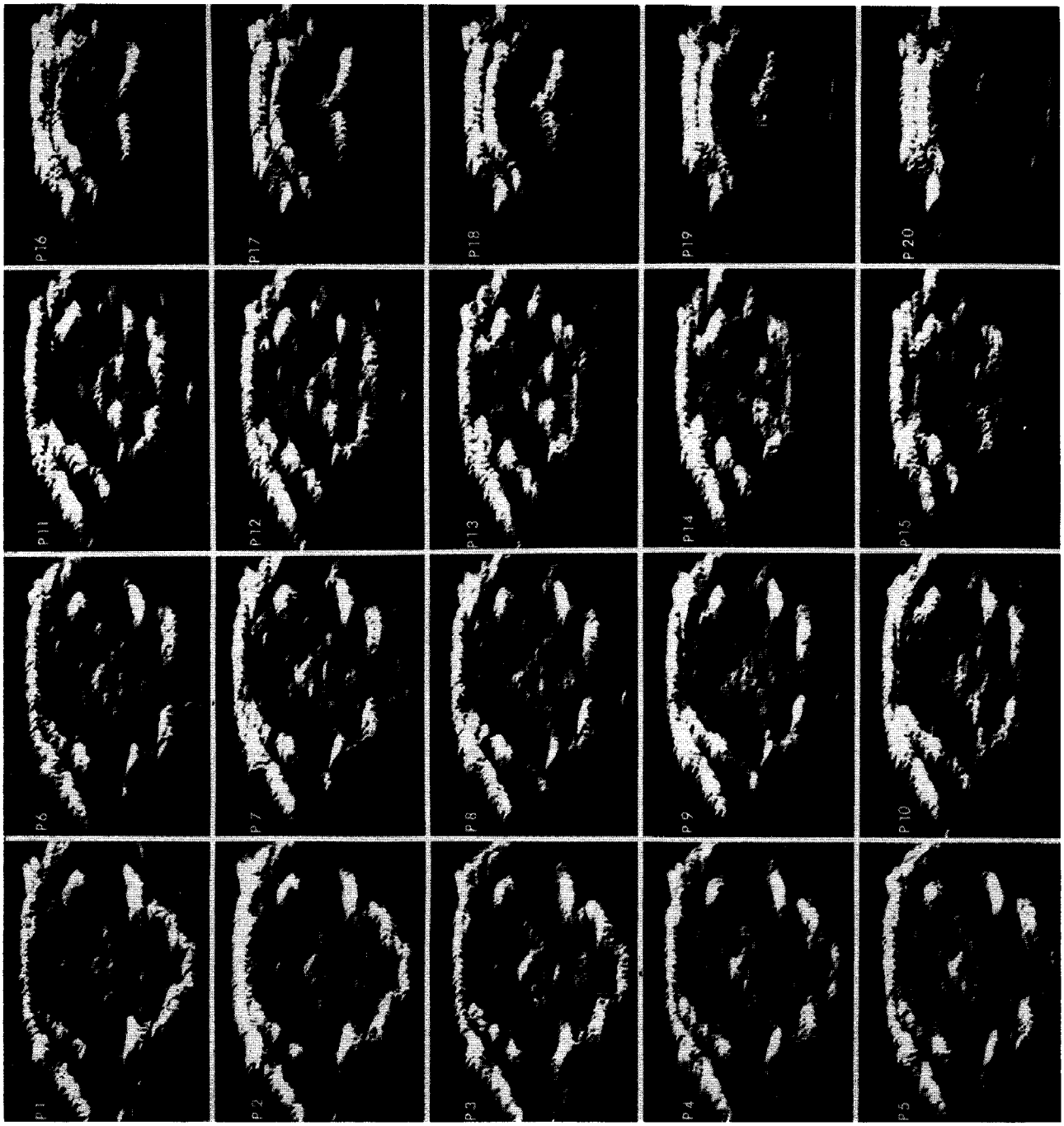

FIG. 7. Echograms of tissue sections throughout the entire anteroposterior extent of the rhesus brain—sector scanning restricted to the plane of section.

to the plane of section. Finally, composite echograms for several different positions in a single animal are shown.

Sixty parallel transverse echograms of the intracranial anatomy of subject G are shown in Fig. 7. The scale, as designated in section A44, is the same for all echograms. The width of the individual bands in these pictures is approximately 8.5 mm. Seven bands are required for the pictures corresponding to the maximum vertical extent of the structures.

Before employing omnidirectional viewing, it is convenient to obtain a set of echograms, such as those in Fig. 7, to orient oneself with respect to major features. A number of bone and brain features are prominent, and serve as landmarks in the determination of the angular orientation of the echograms with respect to cranial atlas sections.[1]

Several features at the base of the brain are apparent immediately. The foramen magnum is seen in echograms P5 to P11 inclusive; the posterior ridge of the body of the sphenoid is detected most posteriorly on A24 and present as a well-developed mass of echoes on A25.* These two features place a series of echograms in approximate correspondence with atlas sections, or skull roentgenograms, of the subject. However, they are not sufficient to determine the angles which the echogram sections make with brain axes, such as the intercommissural line. This angular orientation is determined after identification is made of certain soft tissue features on the echograms. (See appendix.)

The changing form of the anterior cranial fossa is apparent forward from the posterior ridge of the sphenoid at the midsagittal position (compare echograms A32 through A38). The v-shape of the surface contour of the bone medial to the orbits becomes well-developed within an interval of 3 mm—A33 to A36. As the v progressively enlarges vertically, ethmoid bone reflections arise from the base. One might conclude from skull measurements that the transition between sphenoid and ethmoid occurs, for this particular subject, in the neighborhood of A35.

Note, in the anterior echograms of the series, the changing pattern at the base corresponding to emergence of the temporal lobes. First apparent on A31, well-developed on A30, the pattern becomes increasingly massive and ultimately extends medially to abut the echo-pattern of the hypophyseal fossa on A25. This bilaterally-concave echo-pattern, corresponding to the medial cranial fossae, disappears beyond A14 as the patterns develop from the anterior face of the petrosal part of the temporal bone.

At the anterior position of the sphenoid ridge and immediately posterior to it are echoes corresponding to the anterior clinoid processes—A24. These echoes are well-developed above the base of the pituitary fossa, which extends posteriorly to about A17. The dorsum sellae and associated posterior clinoid processes are dense masses on the echograms anterior to A16, in agreement with measurements on skull roentgenograms. Since the interface of bone with soft tissue, or cerebrospinal fluid, is an extremely good reflector, display patterns corresponding to bony features appear spatially-broadened on the echograms, compared with mutually-abutting soft tissues, or soft tissues with body fluids, for equal receiver gain levels.

The dorsum sellae appear to be 5 mm behind the posterior margin (massive echoes on A25) of the sphenoid in the midsagittal position, since there are strong echoes corresponding to the anterior aspect on A20. However, due to spatial broadening at high amplifier gain, one must assume that the actual value is greater than this value—a spatial broadening of about a millimeter is suggested by the appearance of such echoes in the plane of the echogram, and, if this is the case, the distance interval under consideration is approximately 7 mm. Measurements from skull roentgenograms of the subject yield a value slightly less than 7 mm, which is good agreement.

The reflection pattern corresponding to the region behind the dorsum sellae broadens and

* Since the massive *line* of echoes corresponding to the body of the sphenoid disappears rather abruptly at the posterior aspect, identify the posterior ridge of the sphenoid by moving posteriorly from echograms corresponding to positions of the orbital bones.

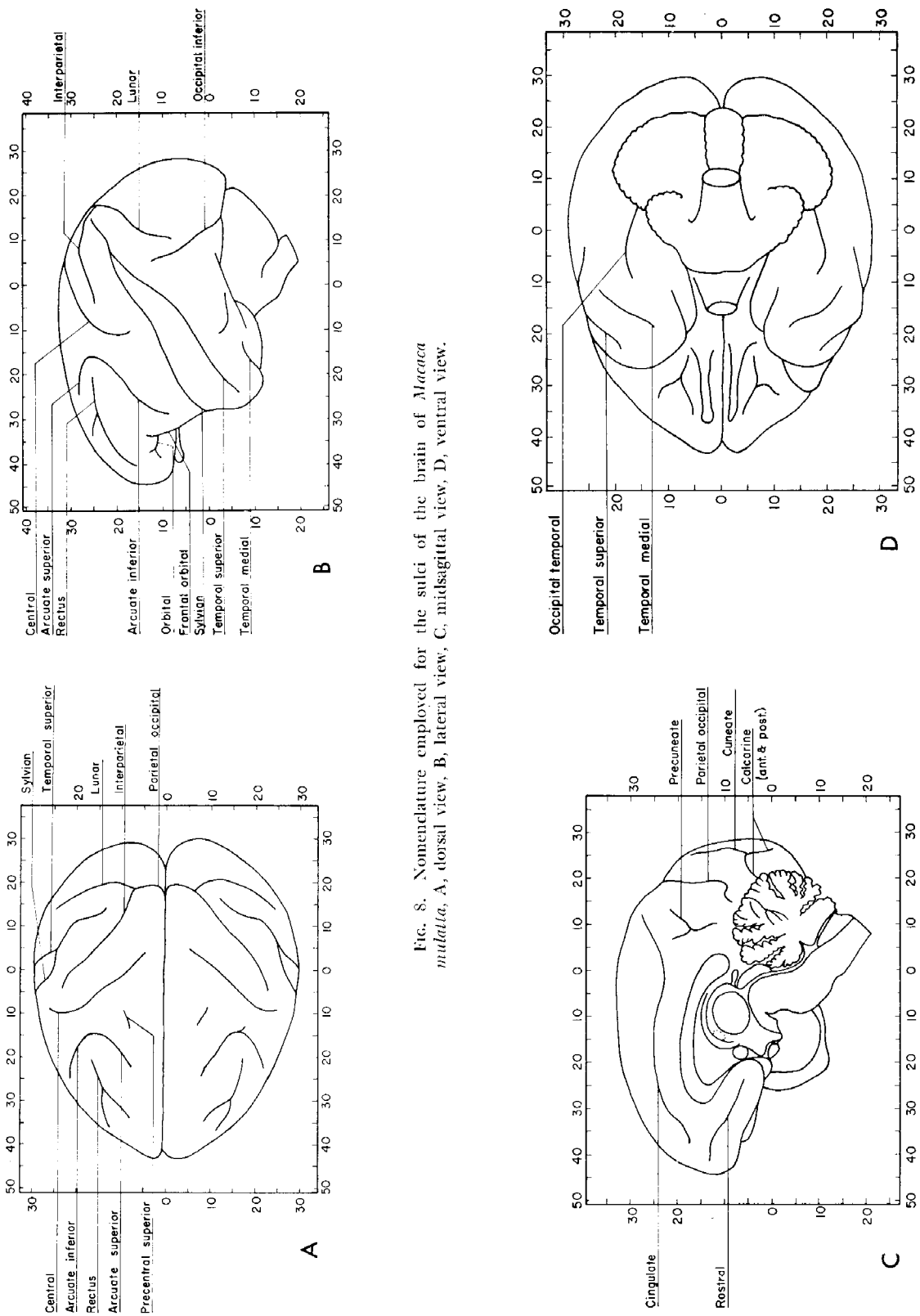

FIG. 8. Nomenclature employed for the sulci of the brain of *Macaca mulatta*, A, dorsal view, B, lateral view, C, midsagittal view, D, ventral view.

becomes somewhat more diffuse posterior to position A16. The echogram is also freer of echoes in this position, which is readily apparent on A14 and becoming evident on A15. This change in pattern corresponds to the petrosal part of the temporal bone, which separates the medial from the posterior cranial fossa. Echoes are received from the anterior face and from the superior ridge of the petrosal bone. Because of the angle of incidence involved, somewhat less reflected energy is detected, from the part of the sphenoid lying posterior to the dorsum sellae and from the basilar part of the occipital bone lying still farther posterior. The distance between the medial margins of the echoes, corresponding to the superior margins of the petrosal bone, becomes greater posterior from A6 in correspondence with the changing configuration of the skull. At the position of the anterior margin of the foramen magnum, the distance between the most medial echoes is 30 mm—in agreement with skull measurements.

The distance from the anterior aspect of the dorsum sellae to the anterior margin of the foramen magnum is the difference between A20 and P4, minus 1 to 2 mm, for an interval of 21 to 22 mm, in agreement with roentgenogram measurements.

Moving posteriorly from the foramen magnum, the contour of the echo pattern at the base of the brain conforms with the changing shape of the skull. The bilateral concave appearance seen in P15 corresponds to echoes from the occipital fossa, and the concavity becomes more apparent posterior to this position, with the echoes from the midsagittal region corresponding to the internal occipital crista, seen on echograms P17 to P19.

Soft tissue features: The apex of the external cortex can be identified by echoes other than those corresponding to the scalp in a major number of echograms of Fig. 7—A33 to A16. The two echo patterns are essentially continuous from A15 to A5, although the position of the cortical surface can be partially distinguished. In the neighborhood of the midsagittal position, no cortical echoes distinguishable from those of the scalp are seen in many more posterior sections until P15 is reached. The lateral aspect of the external cortex surface is clearly defined by echoes throughout most of the brain.

The terminology used in describing the sulci is illustrated in Fig. 8; the sagittal projection diagram of the rhesus brain (Fig. 15) is the base for discussing distance relations quantitatively. The Appendix includes a method for determining the relative orientation of reference atlas and echogram cross-sections, and the scaling factor relating their spacing intervals.

Note in A33 that the cingulate sulcus appears as a strong reflection. This sulcus is manifested as a strong signal on all echograms as far as A7 but further on (to A1) the echoes are weaker. Anterior to A33 the sulcus is apparent as a strong signal that can be followed to A42. Posteriorward from A8 the echo corresponding to the cingulate sulcus approaches the apical cortex, and at A4 lies only 3 mm below it. This behavior corresponds to the configuration of this sulcus (Fig. 8C).

The precuneate sulcus, apparent below the cingulate by 6 mm on A2 and A1, is present as a strong signal on 0, and continues to be present on P1 through P5.

Returning to A33, the reflection lateral to the midsagittal position by 10 mm and ventral to the cingulate sulcus by 5 mm corresponds to the rectus sulcus. Echoes corresponding to this sulcus are present on A34 and faint on A36 and A32. These echoes correspond to the rectus sulcus, as is apparent from the measurements indicated, and because they lie in the appropriate vertical position between echoes corresponding to the arcuate superior and arcuate inferior sulci (A27). Echoes from these latter two sulci on the lateral aspect of the brain appear on a number of echograms (Fig. 8B). The arcuate superior appears on the right side on A25 through A27, and the arcuate inferior appears on A26 faintly, on A27 and A28, and probably on A29. On the left side, the arcuate inferior is manifested strongly on A28 and faintly on A27 and A26. One does not, in general, expect to see the sulci symmetrically positioned

on both sides of the brain, since the angular orientation of the brain surfaces within the sulci determines whether reflected energy is received and such surface orientations are not constant from one side to the other. To elicit echoes from bilaterally corresponding features omnidirectional scanning would be needed over their entire spatial extent.

One notes on A33 an echo at the midsagittal position approximately 7 mm above the reflection corresponding to the base of the skull. This echo and those in the corresponding position on A32 and A31 arise from the sulcus of the corpus callosum at the ventral surface of the genu. As one moves posteriorly, additional echoes are apparent in the midsagittal position 6 to 6.5 mm above the ones just discussed. These correspond to reflections from the sulcus of the corpus callosum at the latter's dorsal surface. The sequence of strong echoes from this sulcus continues uninterrupted to A16.

Moving from the anterior end the echogram pattern shows details of the lateral ventricular system, which become bilaterally apparent on A25, although echo signals are present as far forward as A29. Posterior from A25, a bilateral pair of echo signals is present on each echogram to position A23, fusing together on A22, and appearing as far as A13.

Another feature, posterior from the frontal part of the brain, is seen on the left side of A24, that is, a group of separated *line segments* centered above the vertical level of the echoes corresponding to the dorsum sellae and about 20 mm lateral to the midsagittal position. This array of echoes, which ranges from A27 to A22, and possibly to A21, corresponds to brain surface details within the depths of the sylvian fissure. The sylvian fissure can be identified in some sections as far as A12. On the right, the anterior part of the series of echograms, which contains patterns corresponding to the sylvian fissure, exhibits only a few isolated echoes which correspond to interfaces within the depths of this fissure. This structure cannot be followed as well as that on the left.

Note on A12 that a line segment of echoes is present on the left 6.5 mm above those from the sylvian fissure. This definitive group of echoes arises from the interparietal sulcus; and relatively strong echoes corresponding to it can be seen in the appropriate positions on A10, A11, and A13, with weaker echo signals appearing on A14 and A15.

About 5 mm dorsal to the interparietal sulcus, on A12, bilateral echoes appear, corresponding to others both anterior and posterior to this position. These correspond to the central sulcus, and echoes corresponding to this same sulcus can be seen bilaterally on A14, A13, and A12, and unilaterally on A11 and A10.

A pair of bilaterally strong echoes appears on A12, above those from the bone surface at the base of the brain. These correspond to the dorsal aspect of the hippocampal gyrus and overlying ventral part of the brain stem, where these structures border the cisterna ambiens. Echoes corresponding to these interfaces can be seen in sections A10, A11 and A13.

On A12, a separation develops between the strong echoes from the lateral ventricles. This echogram, with the two columns of weak echoes adjacent to the midsagittal position, corresponds to a tissue section posterior to the massa intermedia and anterior to the posterior commissure. The interval between the projections of the posterior end of the massa intermedia and the anterior aspect of the posterior commissure along a direction normal to the echogram sections is approximately one millimeter (Fig. 15). Therefore, the strong midsagittal echo manifested on A11, 6 mm ventral to the pattern for the lateral ventricles, corresponds to the dorsal surface of the posterior commissure. Here the bottom of the third ventricle is flattened compared to its more anterior configuration and reflects dorsally incident acoustic energy to excite the examining transducer unit with a strong signal. The corresponding strong midsagittal echo on A10 arises similarly but the echo signal on A11 has a greater lateral extent. Further changes in the echogram pattern are seen more posteriorly and result from moving from the caudal end of the third ventricle into the superior cistern.

The strong lines of echoes astride the midsagittal position on A9, A8 and A7 must arise from the surface of the superior cistern, in accord with the configuration on the midsagittal projection diagram. Evidence for this is the change in vertical spacing between the strong midsagittal line of echoes and those from the lateral ventricles; from essentially 6 mm anterior to A9 to 4 mm on A9—a decrease by one third. This change in dorsoventral spacing interval agrees with atlas data for the anatomic features indicated.

Another feature at the vertical level of the posterior commissure on A11 to A6, is the temporal superior sulcus. It can be seen on the left on all of these echograms and on the right on A9 and A8, definitively, with an indication on A7. It might appear on cursory examination of the echograms that the heavy echoes on the right side on A11 and A10 (a corresponding weaker echo is seen on A12) lying just ventral to those from the sylvian fissure on A13, might correspond to the temporal superior sulcus anterior to positions A9 and A8. However, these heavy echoes are more dorsal in the brain than those corresponding to the temporal superior sulcus seen on A9 and A8, and since they appear on echograms anterior to A9, they should lie more ventral to correspond to the usual course of the temporal superior sulcus. In addition, the echo strength is much greater than that from the sulcus under discussion on the left. These considerations, and the observation that because of their position along the vertical they are unlikely to correspond to the sylvian fissure, suggest that these echoes are caused by an artifact such as a bone fragment.

The echoes on A9, spaced laterally 14 mm apart and lying ventral by 8 mm to the strong group corresponding to superior cistern interfaces, are posterior extensions of patterns described in the third preceding paragraph, but in this cross-section they correspond to the dorsal surface of the anterior lobe of the cerebellum. A comparison of A10, A9, and A8 indicates the locus of separation of the mesencephalon from the pulvinar. Comparison with ant lamella 4 through post lamella 1 of the Clarke-Henderson atlas[1] is particularly useful.* The bilaterally symmetrical echoes, spaced laterally 12 mm apart and lying below the strong echoes from the superior cistern, appearing on A8 (only a faint indication is present on A9 and none on A10) correspond to the anterior end of the calcarine sulcus. This sulcus is well-developed 2 mm posterior to the site of separation, as can be seen from the CH atlas[1]—correspondence between the atlas and the echogram sections in this region approximate: ant lam 1—A7, post lam 1—A5. The lateral spacing on the echograms corresponds to the width of the mesencephalon at the level where it separates from the pulvinar. The pattern of echoes below the level of those from the superior cistern becomes more extensive posterior from A8, and develops into the linear arrays on A5 and A4. From a comparison with post lam 1 of CH, these arrays of echoes apparently correspond to the calcarine sulci and the dorsal aspect of the brain stem which lie at the same vertical level at this position of frontal section in the brain. The midsagittal echo manifested on A5, above the linear array under discussion, then occurs from the posterior pineal.

Strong echoes, recorded in the midsagittal position and ventral to others considered on A5 and A4, must arise from the surface of the fourth ventricle. At and posterior from positions A4 and A3, reflections from cerebellar interfaces become apparent with the presence of the central lobule indicated on A3. The multiplicity of cerebellar interfaces is shown by the complexity of the echogram pattern posterior from A3 to A2 and through P1.

We will not attempt to identify all the pattern detail of echograms corresponding to reflections from the cerebellum. This constitutes a study in itself. Posterior, the bilateral patterns of echo signals, which correspond in A4 to the lateral ventricles, become closely associated with those from the calcarine fissure convolutions. This pattern becomes increasingly complex in more posterior cross-sections.

* Hereafter the following abbreviations are used: Clarke-Henderson atlas—CH atlas; lamella—lam.

This is to be expected from examining the CH atlas sections—the latter's post lam 5, which approximately corresponds, at this vertical level, to echogram A1, lies at the caudal end of the lateral ventricles (post lam 6 passes through the posterior tips). Therefore, most echoes abutting laterally those from the cerebellar convolutions on A1 must result from the calcarine fissure complex. All those echoes at the zero position and further posterior are in this category. The echograms show the increase in dorsal sweep of this fissure—compare P1 with P3 (right side) corresponding to the configuration in the lamella in the CH atlas—compare post lam 5 and 6 with 9 and 13.

The more dorsal echo records of the midsagittal group on P1 and echograms posterior result from the tissue interfaces on the dorsal and dorsolateral boundaries of the cerebellum and the ventromedial boundary of the cerebral hemispheres. The approximately 35° angular orientation of this interface region (e.g., post lam 9 of CH atlas) with respect to the horizontal plane is apparent on P2 through P4.

A5 is the most posterior echogram on which there is a signal corresponding to the sulcus of the corpus callosum; nothing appears in the corresponding positions on A4 or A3. The echo recorded on A5, which is associated with the corpus callosum, lies 13 mm below the external cortical surface, while the midsagittal echo that appears in a similar position on A2 (faintly present on A3) lies 9 mm below the surface. The structure corresponding to this latter echo can be followed from A1 through P5. It remains at essentially the same depth below the external surface, i.e., 9 mm. It is in an appropriate position to correspond to the anterior dorsal branch of the precuneate sulcus, but its course in this brain is more nearly parallel with the external cortical surface rather than oriented as shown in the sagittal diagram.

The sagittal projection diagram suggests that echograms near the zero position, P1 and P2, might exhibit strong echoes from boundaries of the fourth ventricle, and this is the case. On echograms P1 and P2, strong reflection signals are recorded 14 to 15 mm below the dorsal aspect of the cerebellum, and this distance interval agrees with the sagittal diagram for the plane of section and the structural identification indicated.

An interface feature which becomes evident on P4, continues to exhibit its presence on P5, 6, 7 and possibly P8, is the parietal occipital sulcus, lying above the dorsal aspect of the cerebellum. From the sagittal diagram, this sulcus, in its anterior course, runs in the anteroposterior direction approximately perpendicular to the plane of echogram section for a length of about 4 mm before turning dorsally to reach the external cortical surface at the midsagittal position.

On P6 through P8, there is a strong double row of echoes in the midsagittal position, with the lower row approximately 4 mm dorsal to the surface of the occipital bone. Since on P5 the most anterior aspect of the foramen magnum is evident it is concluded that the double-layered echo pattern corresponds to the separation of the dorsal aspect of the medulla and the base of the cerebellum, posterior from the position of the superior recesses of the fourth ventricle. The separation interval is slightly over 2 mm on the sagittal diagram while measurements on echogram P7 indicate the same value.

Posterior from P8, the dorsoventral extent of the cerebellar cross-section apparently decreases—P9 to P11. The vertical *diameter* changes from approximately 13 mm on P9 to approximately 9 mm on P11. Strong echo signals are recorded above the middle of the pattern corresponding to the cerebellum on P10. These extend medially, but not to the midsagittal position on P11 to P14. These prominent echo features correspond to the postclival fissure—see post lam 17 of the CH atlas. Echogram P15 passes through the cerebellum anterior to its posterior end and P16 lies behind the posterior end.

The information identified thus far on the individual echograms is not all that can be detected in each corresponding tissue cross-section, since information obtained employing omnidirectional scanning, specifically with angular orientations of the beam axis outside

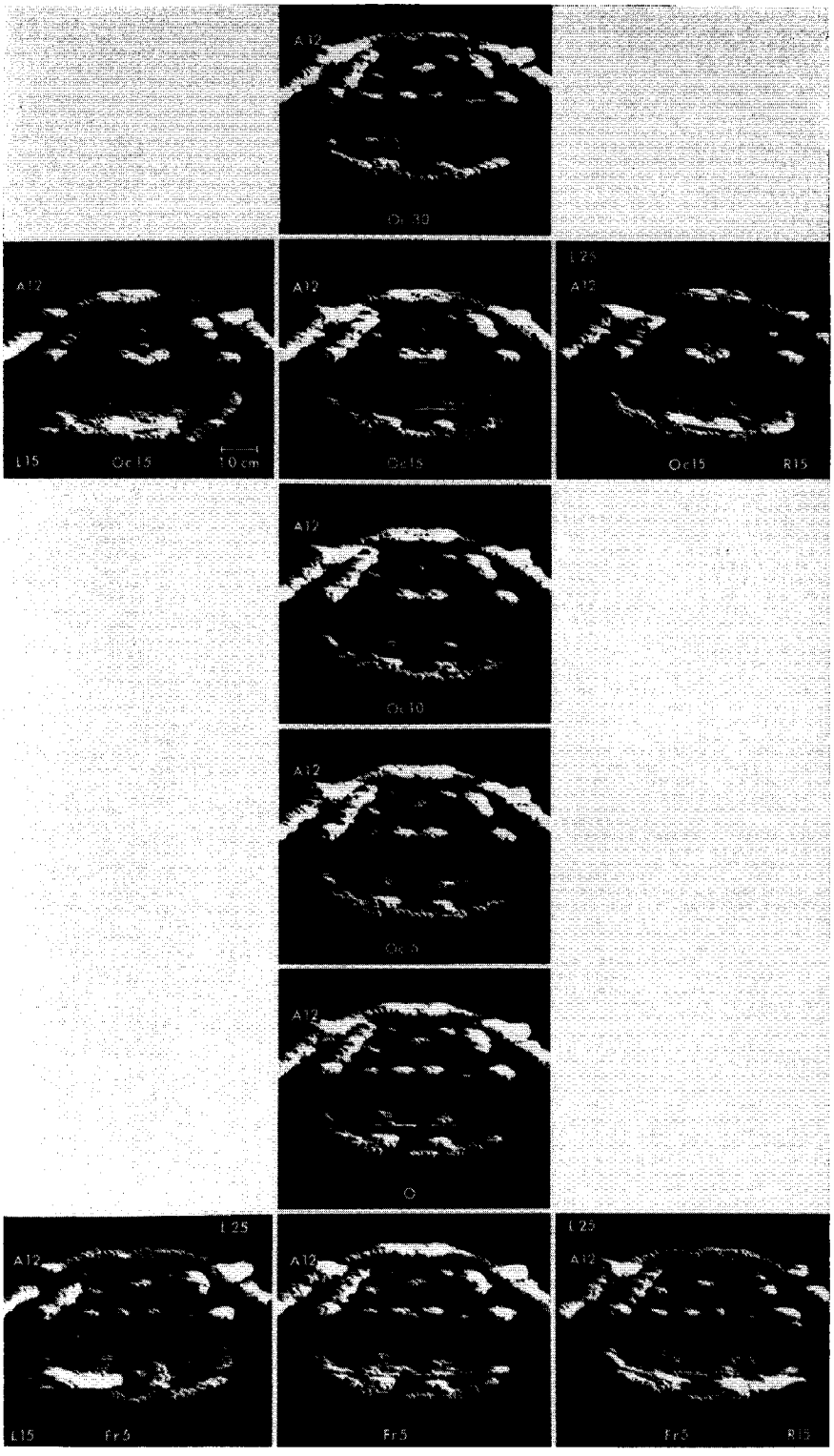

FIG. 9. Echograms at position A12 obtained for various positions of the principal axis of the examining beam.

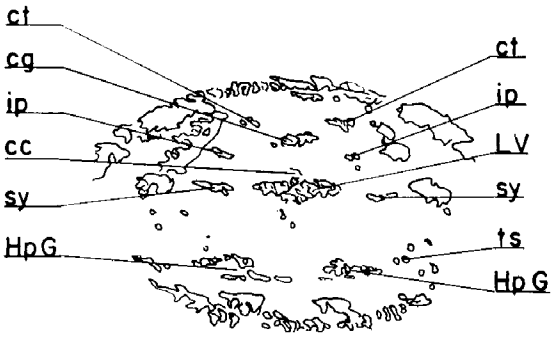

FIG. 10. Composite constructed from the information contained in the echograms at position A12.

the plane of section, has not yet been presented. In addition, all echograms of the series discussed were obtained with sector scanning for a single translational position of the transducer. The remainder of this section of the paper is concerned with omnidirectional scanning. However, for practical reasons only information for sections A12, 0 and P12 is presented.

Echograms corresponding to the tissue cross-section at A12 for different angular orientations and translational positions of the beam axis are illustrated in Fig. 9; the notation on each picture indicates the specific coordinate arrangements. The following additional information is obtained when additional echograms for A12 are compared with the single one in Fig. 7. The echo pattern at the position of the lateral ventricles below the corpus callosum is completed across the midsagittal position when an angular rotation of 15° about the ear bar axis and occipital entry is employed. The curvature of the lateral ventricles in the plane of section is seen in the echograms corresponding to this angle of entry, especially if the principal axis of the examining beam is tilted to the left and right of the midsagittal plane, as in the lateral echograms of the second row. Strong echoes from the sylvian fissure are apparent on the right for the 30° angle of occipital entry, as compared with the less intense and less extensive echo pattern in the section taken with the head in the position of Fig. 7. Other important echoes are detected from the sulcus of

TABLE 1. Abbreviations

Structure	Abbreviation
Cisterns	
Hippocampal gyrus and brain stem bordering cisterna ambiens	HpG
Superior	SC
Miscellaneous	
Anterior cerebellar lobe	CbA
Cerebellar convolutions	CbC
Cerebral hemisphere	CrH
Pineal	
Pineal gland	PG
Sinuses	
Inferior sagittal	infs
Straight	sts
Superior sagittal	spss
Sulci	
Arcuate inferior	ari
Arcuate superior	ars
Corpus callosal	cc
Cingulate	cg
Calcarine	cl
Cuneate	cn
Central	ct
Frontal orbital	for
Interparietal	ip
Lunar	ln
Occipital inferior	oci
Orbital	or
Precuneate (compensatory)	pcn
Parietal occipital (internal)	proc
Sylvian fissure complex	syf
Temporal medial	tm
Temporal superior	ts
Ventricles	
Fourth	IVV
Lateral	LV
Third	IIIV

the corpus callosum in the left and right pictures with an occipital tilt of 15°. Additional features of the hippocampal gyrus are also seen on the figure.

All information in Fig. 9 can be exhibited in a composite, illustrated in Fig. 10. Definitions of all abbreviations in Fig. 10 are given in Table 1. The next tissue cross-section considered is at the zero position, Fig. 11. Echoes are received from fourth ventricle interfaces for a variety of relative orientations of the examining beam axis and the head of the

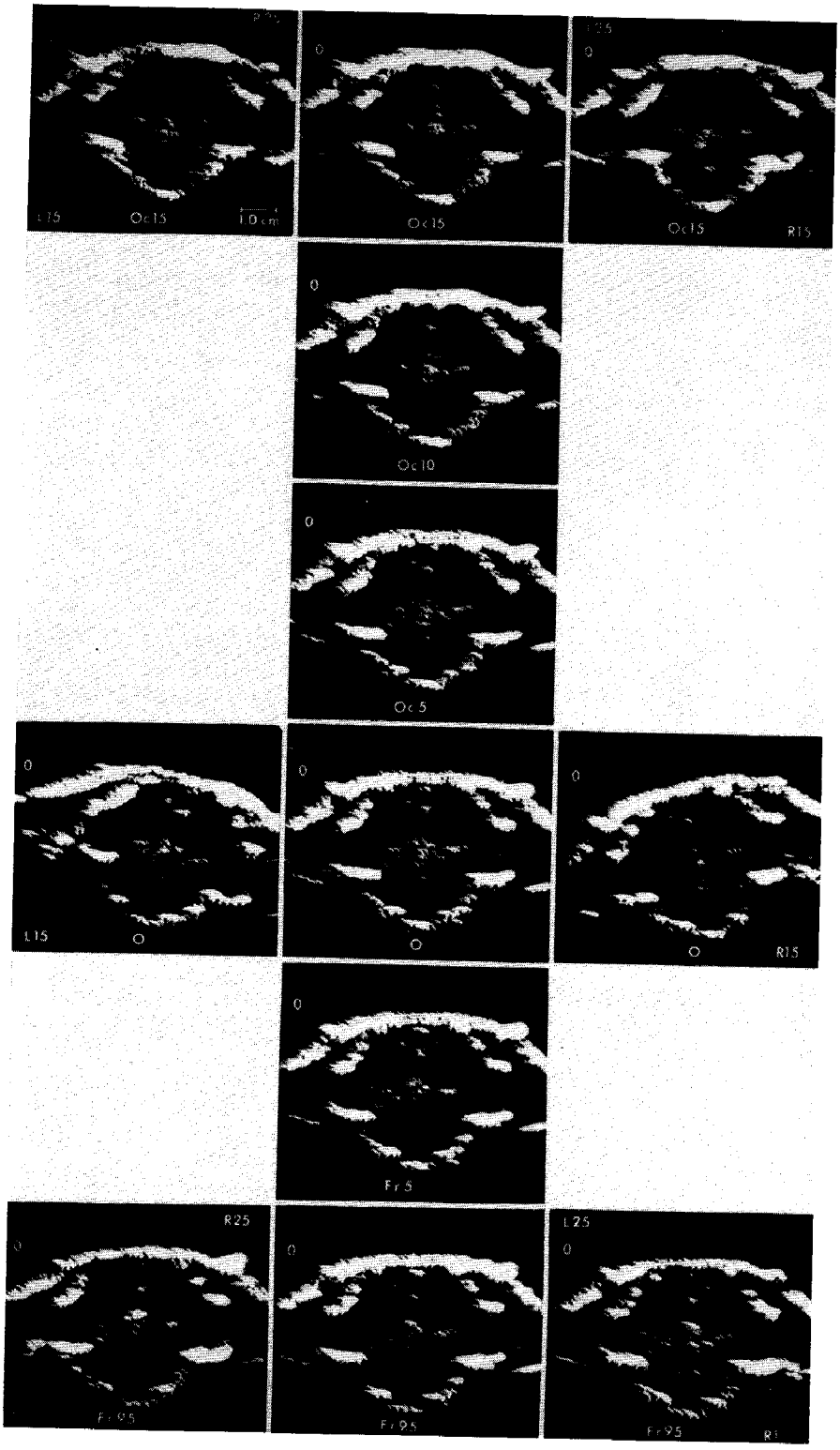

FIG. 11. Echograms at the zero position for various positions of the principal axis of the examining beam.

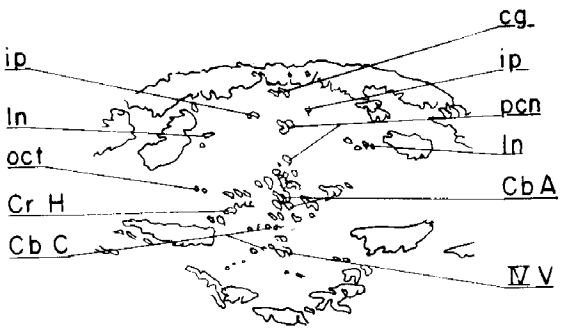

FIG. 12. Composite constructed from the information in the echograms at the zero position.

subject. Stronger echo patterns, to the right of the midsagittal position on some pictures and to the left on others, correspond to those more posterior in sections P1 and P2. Further detail, with respect to the precuneate sulcus on both the right and the left, is on several of the echograms. Discussion of the additional echo information with respect to the external boundaries of the cerebellar mass will be deferred for a later paper. Fig. 12 is a composite of all echogram information of Fig. 11.

A similar study at position P12 is illustrated in Fig. 13, and Fig. 14 is the corresponding composite. Omnidirectional scanning provides additional information about the sulci. The superior sagittal and straight sinuses are clear in some of the echograms. The major subdivisions of the cerebellum, at this longitudinal position in the brain, are well-outlined in this series.

By direct measurement of the intervals between adjacent *spots* corresponding to different structural features it is apparent that resolution capability of 1 mm is achieved and 0.5 mm is approached in some instances. In its present stage of development the localization accuracy of the system for structures in the brain, under the conditions employed, is thus conservatively ± 0.5 mm. That this localization accuracy for ultrasound can be achieved from brain to brain is substantiated by the production, using focused ultrasonic energy, of small discrete lesions in experimental animals. The experience of the author and collaborators with thousands of cases demonstrates that a geometric placement accuracy of a few tenths of a millimeter is obtainable with appropriate instrumentation.

The resolution indicated can be achieved both in azimuth and in range, using the present transducer units, excitation pulses, signal amplifiers and display circuitry. All echogram information significant from the macroscopic viewpoint is the result of reflections at bone surfaces and soft tissue interfaces with cerebrospinal fluid or blood. A wide range of echo amplitudes corresponding to these interfaces is received. No indication of definitive echo patterns corresponding to gray–white matter interfaces within the brain has been obtained; and these latter features cannot be detected and identified by simply increasing the sensitivity of the system. On increasing sensitivity areas of the echogram become filled with *signals* which exhibit no significant correlation with gray–white matter boundaries. This does not imply that such *signals* have no significance, as yet unidentified, but their distribution does not correspond to recognizable features of macroscopic anatomy.

Summary

The results demonstrate the capability of a recently developed ultrasonic visualization system for detecting features of intracranial anatomy and for displaying this information in the form of planar cross-sectional views of (1) internal features of the cranial vault; (2) boundary configurations of ventricles, cisterns, sulci and fissures; (3) major blood vessels such as midsagittal sinuses—under the condition that the acoustic energy does not traverse bone. The introduction of increased sophistication in (1) scanning (omnidirectional viewing), (2) individual echogram composition (program control of signal amplification and picture construction); (3) presentation (relief display); and (4) data processing for echogram superposition (composite overlays), provides considerable advantages over other forms of ultrasonic visualization instruments with respect to the acquisition of anatomic information, including: a greater amount of structural data, uniform resolution

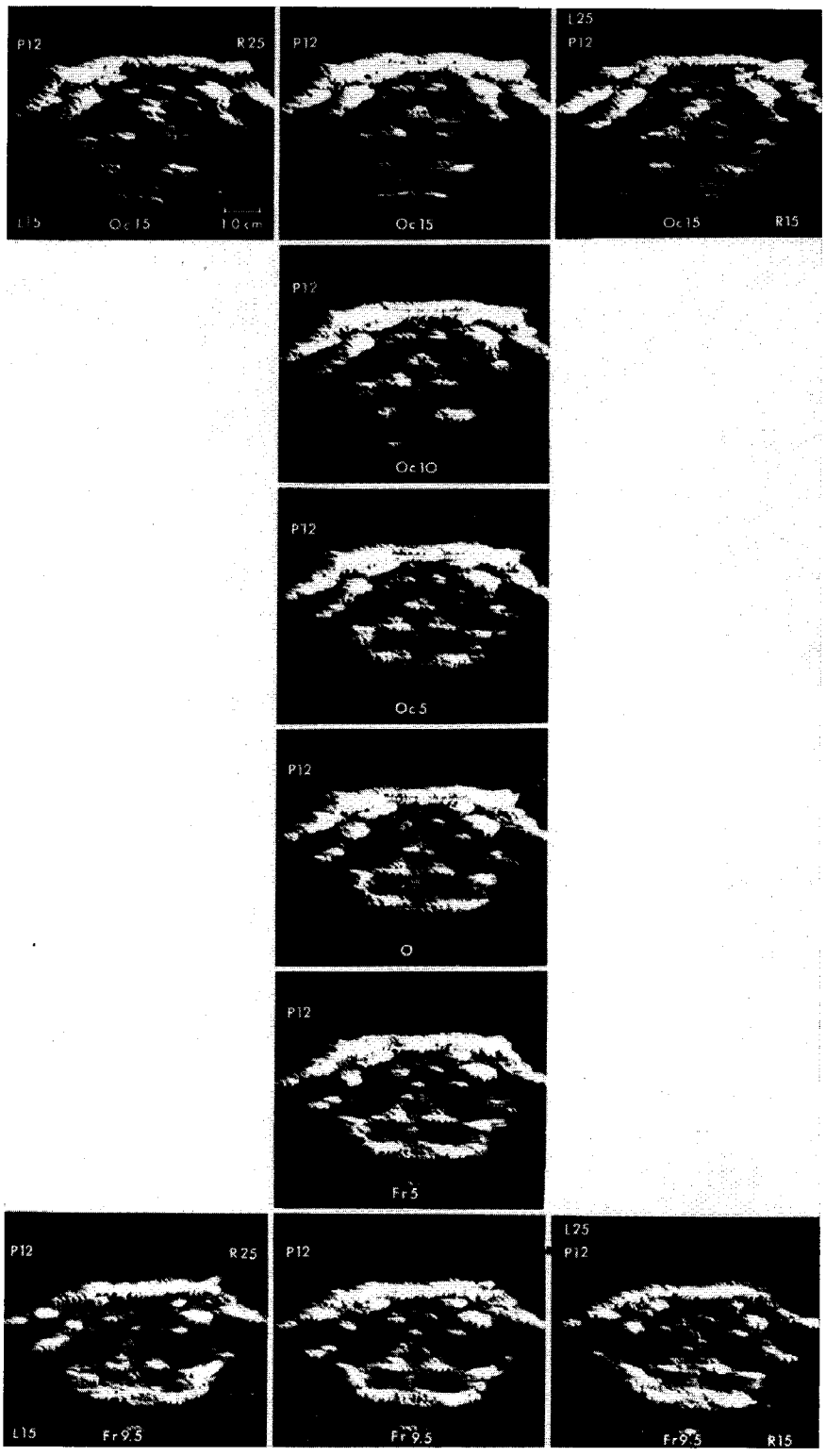

FIG. 13. Echograms at position P12 for various positions of the principal axis of the examining beam.

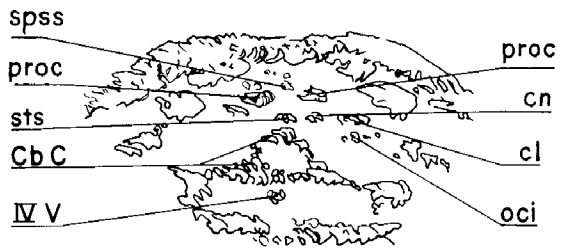

FIG. 14. Composite constructed from the information in the echograms at P12.

over echograms of entire brain cross sections, improved capability in detection of significant echoes, easier assimilation of echogram pattern information by the viewer, presentation of additional characteristics of echo signals. Omnidirectional scanning is essential for any detailed ultrasonic examination of the brain. Only by employing the additional angular degree of freedom characteristic of this type of scanning is it possible to obtain sufficient echo information to permit visualization of the contours of many anatomic features in a comprehensive fashion.

Rhesus monkeys prepared with a large window in the skull but with the scalp intact have been the subjects in the development of the new instrumentation facilities and methods. A resolution capability of 1.0 mm and an accuracy of localization of ± 0.5 mm are achieved throughout the entire intracranial tissue mass for the values of the operating parameters employed.

All definitive signal patterns in the echograms, at sensitivity levels where the echogram is not simply filled with a dense distribution of spots have been correlated with anatomic features. No echogram patterns that correlate in a unique manner with gray–white matter interfaces have been elicited. When the sensitivity for echo detection is increased, many additional signals appear in the display; some correspond to positions where gray–white matter interfaces are located, others where such interfaces are definitely not present.

Methods of determining the value of a scaling factor for comparing the spacing intervals between atlas cross-sections and subjects' echograms and their relative angular orientations are described and illustrated.

The advantages of a general purpose on-line digital computer in a sophisticated and versatile ultrasonic visualization facility for examining the brain have become strikingly apparent during the course of our work.

Address for correspondence: William J. Fry, Interscience Research Institute, Interstate Research Park, P.O. Box 318 Country Fair, Champaign, Ill. 61820

REFERENCES

1. Clarke, R. H., and E. E. Henderson: Atlas of Photographs of the Frontal Sections of the Cranium and Brain of the Rhesus Monkey. *Johns Hopkins Hospital Reports* **Suppl. 19**, Part II, 1920.

2. ———: Investigation of the Central Nervous System—Methods and Instruments. *Ibid.*, Part I, 1920.

3. Fry, W. J., G. H. Leichner, D. Okuyama, F. J. Fry and E. Kelly: Ultrasonic Visualization System Employing New Scanning and Presentation Methods. In press.

4. Grossman, C. C., J. H. Holmes, C. Joyner and E. W. Purnell, eds: Diagnostic Ultrasound—Proceedings of the First International Conference, University of Pittsburgh, 1965. New York, Plenum Press, 1966.

5. Grossman, C. C.: A and B Scan Sonoencephalography (SEG)—A New Dimension in Neurology. *Ibid.*; p. 130.

6. Olszewski, J.: The Thalamus of the Macaca Mulatta—An Atlas for Use with the Stereotaxic Instrument. New York, S. Karger, 1952.

7. White, D. N., J. M. Clark and M. N. White: Studies in Ultrasonic Echoencephalography VII—General Principles of Recording Information in Ultrasonic B and C Scanning and the Effects of Scatter, Reflection and Refraction by Cadaver Skull on this Information. *Med. Biol. Illus.* 5:3, 1967.

APPENDIX

It is useful, from the viewpoint of enhancing the speed of interpretation of echograms, to compare them with brain atlas cross-sections and it is desirable to determine accurately the relative angular orientation between the tissue cross-sections and those of the atlas. It is essential to calculate the factor(s) relating the scales of the atlas coordinates to those of the brain under examination. Both of these can be evaluated by identifying a series of definitive anatomic features on the echograms and then indicating their corresponding positions and anteroposterior coordinate values on the sagittal projection diagram corresponding to an atlas, as illustrated in Fig. 15. An atlas and corresponding sagittal projection diagram, with bony features included, is more useful than the diagram of the figure and the Olszewski atlas;[6] however, this combination was not available when these studies were made.*

* A sagittal projection diagram could be prepared from the Clarke-Henderson atlas to provide the desired combination.

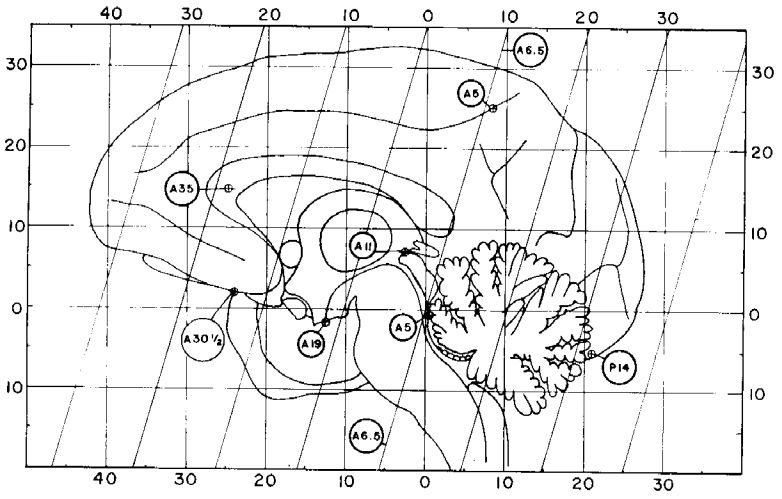

FIG. 15. Sagittal projection diagram of rhesus brain adapted from Olszewski.[6] Orientation of echogram sections is shown together with the locations, determined from the echograms, of certain specific anatomic sites in the brain of the subject.

A convenient set of anatomic features for the indicated purpose follows (the specific coordinate values refer to the subject of Fig. 7):

1. Approximate position of anterior disappearance of echoes from sulcus of corpus callosum for examining beam orientation employed—A35;

2. Anterior end of temporal lobes at level of base of frontal lobe—A30½, the average of A30 and A31;

3. Anterior aspect of the dorsum sella—A19;

4. Anterior dorsal aspect of posterior commissure—A11;

5. Cingulate gyrus at the longitudinal position where its course lies halfway between the external cortical surface measured from its deepest position below that surface—A5 (dorsal);

6. Reflection from roof of rostral end of fourth ventricle—A5 (ventral).

All the above sites are not without some ambiguity in the coordinate values ascribed to them, and all would not be uniformly useful in examining all subjects. Also, as more experience is obtained, others could prove more useful than some of these. The accuracy of the coordinate determination could be improved in many cases by examining the region of each site by omnidirectional scanning. This has not been done in our study, since the goal has been the demonstration of the capability of the facility and methodology, and there has not been time to refine some aspects of the method as suggested by the analysis of the most recent data.

The next step, in the procedure for determining the scale factor and the relative orientation, is to read the atlas coordinates, anteroposterior and dorsoventral, for each of the anatomic features listed above and designated on the sagittal diagram. It is possible to determine the scale factor from a graph of the anteroposterior coordinate value for the subject, as a function of the corresponding atlas coordinate, Fig. 16, for those sites lying close to a single horizontal plane of the atlas (A30½, A19 and A5 [ventral]). When a straight line is drawn through these three points, its slope is 1.00. Since the ratio of the distance interval in the subject to that of the atlas is equal to this slope, the anteroposterior scale factor is thus determined. Another quantity yielded by the graph is the echogram coordinate number that corresponds to the zero of the anteroposterior coordinate value of the atlas—from the figure this value is A6.5.

The other sites, which are some distance from the reference plane, are also indicated on the

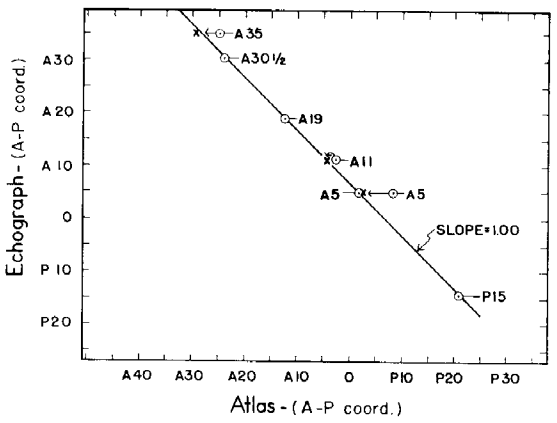

FIG. 16. Graph of anteroposterior (AP) coordinate of the subject as a function of the corresponding atlas coordinate.

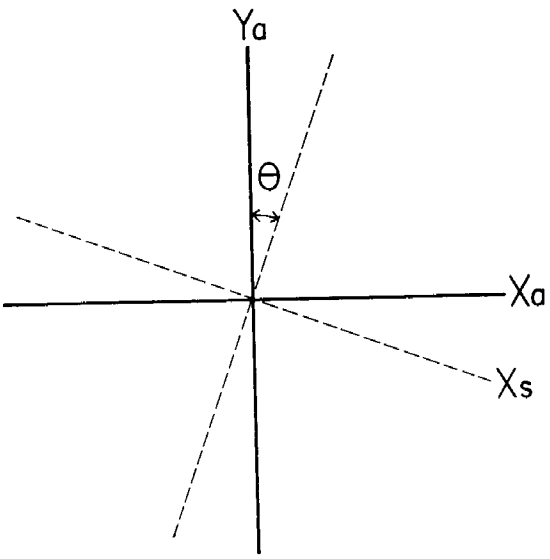

FIG. 17. Notation employed for designating rectilinear coordinates of atlas and subject and the angular displacement between the two systems.

graph since they serve to confirm the consistency of the method when their anteroposterior coordinate values are modified to project them, by the method described later, to the dorsoventral level of the horizontal reference plane after the relative angular orientation of subject (echogram) and atlas sections is determined.

The relative angular orientation between the subject and atlas coordinate systems, i.e., the angle θ of Fig. 17, is calculated from well known transformation formulas. The symbols in the expression presented here have the following meanings:

x_s = anteroposterior subject coordinate value of anatomic site minus subject coordinate value corresponding to the zero reference of the atlas—if subject coordinate value is preceded by A, negative sign is employed, if by P, positive sign is used;

x_a = anteroposterior atlas coordinate value of anatomic site—negative if anterior to zero reference and positive if posterior to this reference;

y_a = dorsoventral atlas coordinate value of anatomic site—negative if ventral to horizontal reference plane and positive if dorsal to reference plane.

The expression for calculating θ is:

$$\sin \theta = \frac{-x_s y_a \pm x_a \sqrt{x_a^2 + y_a^2 - x_s^2}}{x_a^2 + y_a^2},$$

where the plus sign is employed if y_a is positive and the minus sign is used if y_a is negative. The sign convention considers rotation of a line directed in the positive sense of x_a, clockwise to coincide with the positive sense of x_s, as a positive value for θ, whereas if counterclockwise rotation is required, the value of θ is considered negative. When the coordinate values for the three anatomic features, A35, A11 and A5 (dorsal) are inserted into the expression, the three values 16°, 17°, and 15.5° are obtained for θ. A value for θ can only be determined with reasonable accuracy if the anatomic sites employed are at some distance from the reference plane, since a given uncertainty produces an increasingly larger fractional error as the distance of the site from the reference plane becomes smaller.

Generally, calculated values for the angle θ can cover a wide range because of one or both of the following factors: (1) uncertainty in the determination of subject coordinate values for specific anatomic features; (2) a single precise value for the relative angular orientation between subject sections and atlas cross-sections is generally not applicable for the entire brain or a major portion thereof. However, presence of the latter factor does not eliminate the usefulness of a value for the angle of relative orientation, since the placement of the set of echogram sections in the coordinate system of an atlas has considerable utility with respect to the rapid identification of anatomic features corresponding to many of the details of the patterns seen on the echograms, even though the correspondence may be only approximate.

The average of the above three values of θ is 16° and a set of lines corresponding to this relative orientation of the subject and atlas sections can be placed on the sagittal diagram of Fig. 15 as indicated. These coordinate lines facilitate interpretation and examination of additional features of the echograms. It is now possible to correct the atlas coordinate values on the graph of Fig. 16 for those anatomic sites not near the reference plane by projecting the points to the reference plane along the direction of the slant lines, and, when this is done, the shifts of position indicated on the graph result. The shifted points lie essentially on the line determined by the coordinates of those sites close vertically to the reference plane, i.e., A30½, A19, and A5.